

# **Thermal Conductivity of Suspensions of Carbon Nanotubes in Water**

M.J. Assael<sup>1,4</sup>, C.-F. Chen<sup>2</sup>, I. Metaxa<sup>1</sup>, W.A. Wakeham<sup>3</sup>

<sup>1</sup> Chemical Engineering Department, Aristotle University, Thessaloniki 54124, Greece. E-Mail: assael@auth.gr

<sup>2</sup> MER Corporation, 7960 S. Kolb Road, Tucson, Arizona 85706, USA. E-Mail: chen@mercorp.com

<sup>3</sup> University of Southampton, Highfield, Southampton SO17 1BJ, U.K. E-Mail : vice-chancellor@soton.ac.uk

## **ABSTRACT**

The enhancement of the thermal conductivity of water in the presence of Carbon-Multiwall nanotubes (C-MWNT) was investigated. Sodium Dodecyl Sulfate, SDS, was employed as the dispersant and a 0.6% volume suspension of C-MWNT in water was employed in all measurements. The thermal conductivity was measured with a transient hot-wire instrument built for this purpose, and operated with a standard uncertainty better than 2%. The maximum thermal conductivity enhancement obtained was 38%.

In an attempt to explain the experimental observations a number of micro-structural investigations have been carried out and those results are presented here along with the analysis.

**KEY WORDS:** nanotube; SDS; thermal conductivity; water.

---

<sup>4</sup> To whom correspondence should be addressed

## 1. INTRODUCTION

Since the first report on the synthesis of nanotubes by Iijima [1] in 1991, there has been a sharp increase of scientific interest in the properties of these materials and their possible use. Thus, suggestions have already been made, that they can be employed in a very wide variety of applications such as nanolithography [2], low-friction nanoscale linear bearings [3], electromechanical nanotweezers [4], transistors [5].

The nanotubes that are of interest here, typically consist of graphitic sheets rolled up to the form of multiwalled nanotubes (C-MWNT) with about 20 to 100 annular layers, a mean outer diameter of 20 to 500 nm and a length that extends from a few nanometers to several micrometers. Although they exhibit a number of exotic properties, they are particularly characterized by a very high thermal conductivity. Hence, it has recently been proposed that, in order to overcome poor heat transfer rates in conventional heat transfer fluids, a possibility might be to disperse in it, small amounts of nanoparticles or nanotubes. Such a fluid with nanosolids dispersed in it, is called a "nanofluid". Such materials are, strictly multiphase and for that reason it is thermodynamically incorrect to speak of a property of the assembly since the physical property should refer to a single phase system. However, on an appropriate length scale and from a practical point of view it is legitimate to speak of the property of the assembly. We shall continue this practice in this paper though we note that strictly the property which we shall refer to as the thermal conductivity is, properly an effective property of the multiphase system.

During the last four years the study of the enhancement of the thermal conductivity of nanofluids owing to the presence of nanoparticles, has attained considerable interest. In the particular case of nanotubes, Choi *et al.* [6] studied the enhancement of the thermal conductivity of synthetic poly( $\alpha$ -olefin) oil caused by C-MWNT (mean diameter of about 25 nm and length of about 50  $\mu\text{m}$ , containing an average of 30 annular layers) and found a 2.5 fold increase at 1 vol % of nanotubes. A bare-platinum transient hot-wire instrument was employed for the measurement of the thermal conductivity of the suspension.

In this work we present a detailed study of the thermal conductivity enhancement of water when C-MWNT are added.

## 2. C-MWNT PREPARATION AND CHARACTERIZATION

The C-MWNT employed in this work were produced by MER Corporation, U.S.A., by the Catalytic Decomposition Method. This is one of the most promising techniques for production of nanotubes because it can be operated at atmospheric pressure and moderate temperatures with high selectivity to C-MWNT. Furthermore, this process can be scaled up and used for continuous and semi-continuous production.

To characterize the C-MWNT supplied by MER Corporation, a number of different techniques were employed. High Resolution Transmission Electron Microscopy, HR-TEM, (model JEM 2010 at 200 kV) photographs showed a mean outer diameter of about 100 nm, in a wide distribution of values ranging from 15 to 330 nm. The average number of graphite sheets observed was about 100, while inner diameters ranged from 2 to 30 nm. In Fig. 1, a typical HR-TEM photograph of an 80-nm-outer diameter, 25-nm-inner diameter, consisting of about 100 sheets C-MWNT magnified 800,000 times, is



**Figure 1.** C-MWNT magnified 800,000 times.

shown. The range of diameters observed, was also verified by Conventional Transmission Electron Microscopy, C-TEM (model JEOL 120CX at 100 kV).

Scanning Electron Microscopy, SEM, (model JEOL JSM-6300, 20keV) was also employed to determine the length of the C-MWNT and average lengths over 50  $\mu\text{m}$  were revealed.

### **3. C-MWNT SUSPENSIONS PREPARATION**

When C-MWNT are added in water, they form a non-homogeneous, unstable, suspension with large agglomerates of C-MWNT present locally. Precipitation starts after several minutes. In order to obtain a homogeneous and stable solution, two procedures were adopted. A small amount of dispersant was employed and the

suspension was subjected to ultrasonic vibration. Ultrasonic vibration can however, have two effects, it can break the C-MWNT agglomerates to form a more uniform suspension, but it can also break the C-MWNT themselves to small lengths.

In the present work, to ensure the uniform dispersion of the C-MWNT in water (Reidel-de Haën, CHROMASOLV), Sodium Dodecyl Sulfate, SDS, was employed. A 0.6% volume suspension of C-MWNT in water was employed in all measurements.

Three groups of suspensions were prepared:

- 1) **Group A suspensions.** These were prepared by first adding C-MWNT in water and then SDS. The resulting suspension was placed in an Ultrasonic Homogenizer (model HD 2200 Bandelin Electronics) for a period of time ranging from 10 up to 180 min.
- 2) **Group B suspensions.** These suspensions were formed by decreasing the water content of other suspensions by evaporation. The resulting suspension was placed again in the Ultrasonic Homogenizer for a period of time ranging from 70 to 320 min.
- 3) **Group C suspensions.** These suspensions were formed by "regenerating" the C-MWNT from older suspensions, with successive treatments of centrifugation, homogenization and drying. The total ultrasonic homogenization duration ranged from 430 to 500 min.

After a set of points of constant SDS content was obtained, more SDS was added in the solid form and the specimen was again subjected to ultrasonic homogenization.

Optical observation showed indeed as expected that increasing the concentration of SDS produced more homogeneous suspensions of the C-MWNT. Similar effect was observed when increasing the homogenization duration. Hence, in addition to the measurement of the actual enhancement of the thermal conductivity of these suspensions, the impact of the

- effect of the concentration of the dispersant SDS, and
  - effect of the homogenization time
- need also to be investigated.

## 4. C-MWNT SUSPENSIONS CHARACTERIZATION

In order to characterize the suspensions whose thermal conductivity was to be measured, Scanning Electron Microscopy, Fourier Transform Infra-Red Spectroscopy, and Micro-Raman Spectroscopy were employed.

### 4.1. SEM results

Scanning Electron Microscopy, SEM (model JOEL JSM-6300, 20keV), was employed on the following four typical suspensions:

- 1) Suspension 0.1% wt. SDS (Group A), 20 min homogenization.
- 2) Suspension 0.5% wt. SDS (Group A), 120 min homogenization.
- 3) Suspension 2.0% wt. SDS (Group B), 320 min homogenization.
- 4) Suspension 0.5% wt. SDS (Group C), 490 min homogenization.

All samples were coated with gold. A 0.6% volume suspension of C-MWNT in water was employed. The results of the examination of the samples are given below.

#### 4.1.1. Suspension 0.1% wt. SDS (Group A), 20 min homogenization

In this suspension, C-MWNT agglomerates can be seen, with sizes up to 1.5  $\mu\text{m}$ . Nevertheless, this is a stable specimen with a uniform network, with nanotube lengths more than 70  $\mu\text{m}$ , as it can be seen in Fig. 2. A careful observation reveals that the sample contains nanotubes with a wide variation of diameters, which however, are uniformly spread. It should also be noted that in this suspension, there are some botryoidal formations of carbonaceous material (verified by x-ray analysis), which are also found throughout the whole specimen.

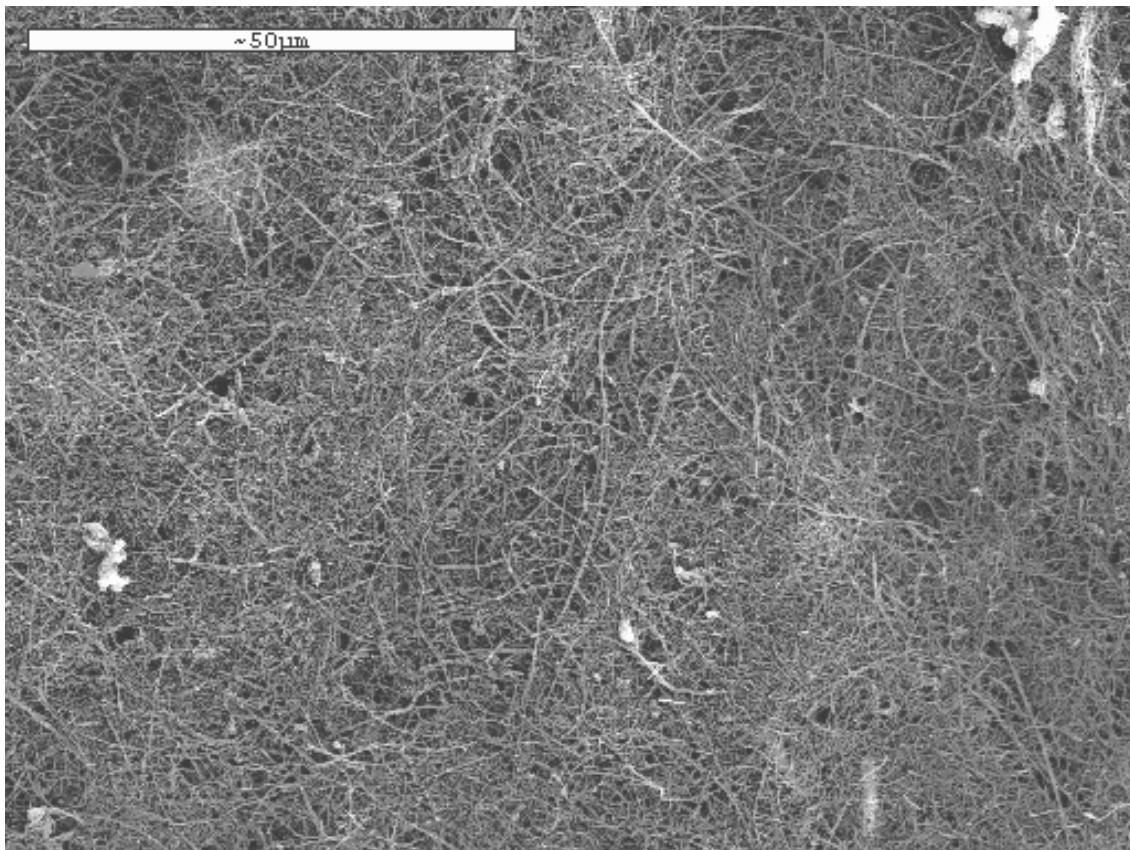


**Figure 2.** Suspension 0.1% wt. SDS (Group A), 20 min homogenization - magnified 1000 times.

#### 4.1.2. Suspension 0.5% wt. SDS (Group A), 120 min homogenization

In this suspension, agglomerates can clearly be seen, with sizes up to 1 mm. Nevertheless, this is a homogeneous suspension, as it can be seen in Fig. 3. Furthermore, it can be seen that the sample consists mainly of nanotubes with lengths greater than 50  $\mu\text{m}$  (at the center of Fig. 3) with only a few nanotubes with lengths less than 5  $\mu\text{m}$  (down at the left side of Fig. 3). The diameters vary from 30 nm to more than 300 nm.

In this sample we also observe formations, that x-ray analysis showed to be mainly C, along with admixtures of Ti and Al.

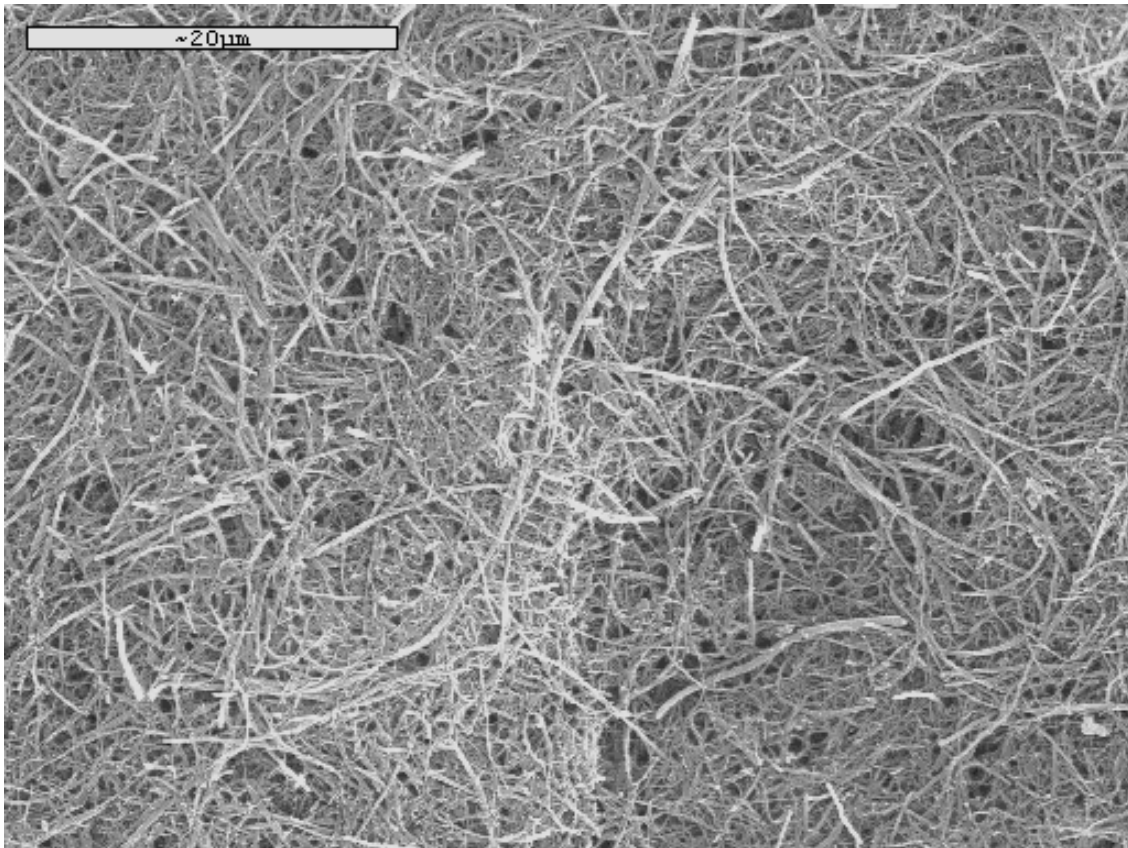


**Figure 3.** Suspension 0.5% wt. SDS (Group A), 120 min homogenization - magnified 1900 times.

#### 4.1.3. Suspension 2% wt. SDS (Group B), 320 min homogenization

This sample resembles a black-color liquid with no visible agglomerates. It is uniform and consists of well-dispersed nanotubes of small length (mean length less than 5  $\mu\text{m}$ ) as shown in Fig. 4. A closer look reveals that there are different diameters and lengths as small as 1  $\mu\text{m}$ . Hence, this is a uniform sample with nanotubes that have been ‘broken’ to smaller lengths, due to the treatment with the ultrasonic vibrator.

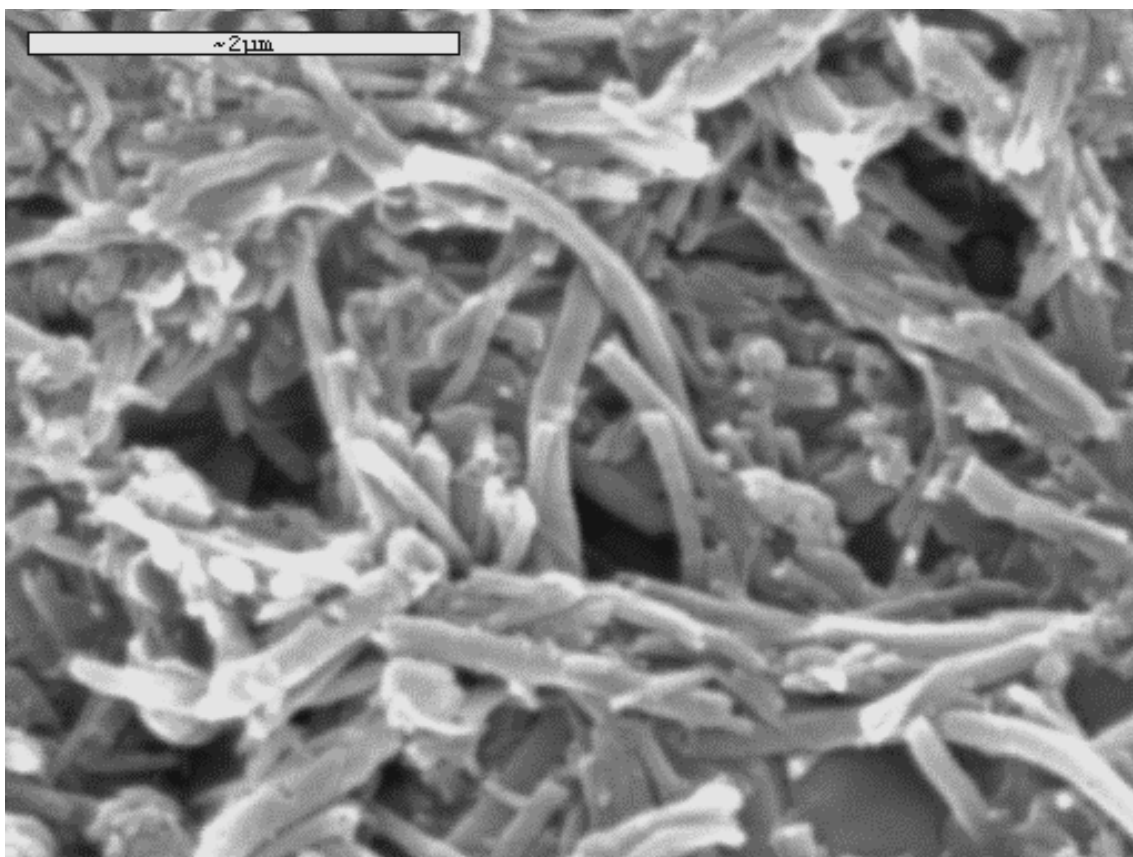


**Figure 4.** Suspension 2.0% wt. SDS (Group B), 320 min homogenization - magnified 22000 times.

#### 4.1.4. Suspension 0.5% wt. SDS (Group C), 490 min homogenization

This sample is not as stable as the previous samples, because the nanotubes form a separate bulk phase and precipitate more quickly. Nevertheless, for as long as it remains stable, this suspension is uniform and consists of well-dispersed nanotubes of small length, as shown in Fig. 5. It has the same dispersion and form everywhere, independently of the magnification of the image. There are nanotubes with diameters ranging from 30 nm to 250 nm and with a mean length less than 3  $\mu\text{m}$ .

The uniformity of this sample is notable. It must be attributed to the fact that the nanotubes were subjected to the regeneration procedure, which involved centrifugation

and treatment with ultrasounds. The nanotubes were worn out during the regeneration process and they looked like a powder afterwards, thus indicating that they ‘broke’. This experimental observation agrees with the SEM images. We have a uniform suspension of nanotubes with very small lengths.

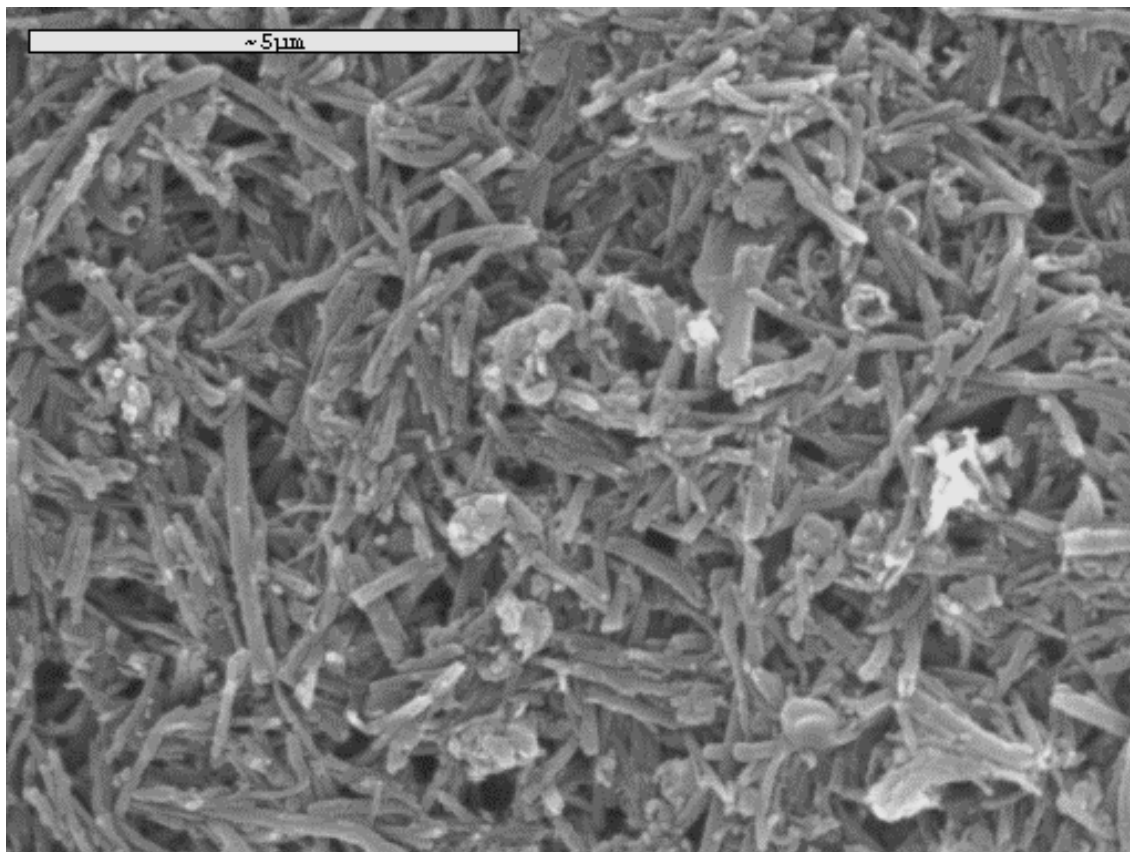


**Figure 5.** Suspension 0.5% wt. SDS (Group C), 490 min homogenization - magnified 10000 times.

## 4.2. Spectroscopic results

### 4.2.1. *Fourier Transform Infra-Red Spectroscopy*

Fourier Transform Infra-Red (FTIR) Spectroscopy, yields information about the type of bonds and the chemical structure of small molecules. This method was employed to investigate the bonds that may be formed between the carbon nanotubes and the surfactant SDS. For this study a phasmatophotometer (model Perkin Elmer 2000) was employed. It has constant nitrogen flow and it is equipped with a detector MCT for the investigation of a wide area of spectrum. After collecting the interferogram, the spectrometer computer uses the Fourier Transform and yields a plot of intensity against frequency ( $\text{cm}^{-1}$ ).

A specimen consisting of 0.6 % vol. C-MWNT and 1.1 % wt. SDS in water subjected to 60 min of ultrasonic treatment was examined. As the concentration was not too high, the resulting peaks were not so clear or intense and thus, could not be identified. Hence, no useful information was obtained so far.

#### 4.2.2. Micro-Raman Spectroscopy

The inability of the FTIR technique to provide results concerning the bonds between the sample components led us to another technique used for identification and analysis, the Micro-Raman Spectroscopy. It is similar to FTIR, but it has the advantages that no special sample preparation is required.

In order to conclude whether SDS forms any kind of bonds with the nanotubes, several samples were studied. Pure nanotubes were examined, to get a base for comparison for the peaks observed in the Raman spectrum. The spectra of three suspensions were taken, with increasing weight ratio of SDS to C-MWNT. These concentrations were chosen, so the influence of the SDS content could be evaluated. The examined samples were (ratio is, % wt. SDS over % wt. C-MWNT) :

- a) C-MWNT bulk (ratio 0)
- b) 0.35 % vol. C-MWNT + 0.6 % wt. SDS (ratio 0.86)
- c) 0.6 % vol. C-MWNT + 0.1 % wt. SDS (ratio 0.08)
- d) 0.6 % vol. C-MWNT + 2.0 % wt. SDS (ratio 1.67)

The suspensions were studied both as a solution and nearly dried. Two laser beams were used, with 514.5 nm and with 647 nm of wavelength respectively. All tests led to similar results. Three peaks are observed.

1<sup>st</sup> peak: It is due to the vibrations of the outside graphitic sheets of the nanotubes. It is affected by the wavelength of the used laser.

2<sup>nd</sup> peak: It is due to the vibrations of the hexagonal graphitic sheets.

3<sup>rd</sup> peak: It is a side peak worth to be further investigated.

The observed peaks for the four samples are given in Table I:

**Table I.** The Raman peaks.

Sample	Weight ratio	1 <sup>st</sup> peak	2 <sup>nd</sup> peak	3 <sup>rd</sup> peak
a	0	1330	1581.6	1619
b	0.857	1355	1582.5	1635
c	0.083	1358	1582.0	1670
d	1.67	1350	1581.0	1607

The reported results are very interesting, since they show that there is interaction of the surfactant SDS with the C-MWNT. In more detail, we conclude that

1<sup>st</sup> peak: It is not the same for bulk C-MWNT and suspension. The values are known with an uncertainty of  $\pm 3 \text{ cm}^{-1}$ . The Raman shift reaches maximum in the dilute suspension and then decreases with increasing weight ratio. This indicates that the vibrations of the outside graphitic sheets of the nanotubes are affected by the presence of SDS.

- 2<sup>nd</sup> peak: It is the same for bulk C-MWNT and suspension. The values are known with an uncertainty of  $\pm 3 \text{ cm}^{-1}$ . The vibrations of the hexagonal graphitic sheets are not affected by the presence of SDS.
- 3<sup>rd</sup> peak: It is not the same for bulk C-MWNT and suspension. The values are known with an uncertainty of  $\pm 10 \text{ cm}^{-1}$ . The Raman shift reaches maximum and then decreases. This indicates that the nanotubes are affected by the presence of SDS.

It is pointed out that other research groups have also reported these peaks. The 1<sup>st</sup> peak is reported by Zhao and Ando [7]. Several groups found the 2<sup>nd</sup> peak, since it is the most characteristic [7, 8, 9]. The 3<sup>rd</sup> peak is mentioned only by Zhao and Ando [7], but for a carbon allotrope which is a side product of C-MWNT (outer shell of the cathode deposit in production by hydrogen arc discharge method).

Hence, it is noted that the Raman spectra of the pure nanotubes and their suspensions lead to a very important conclusion. **The C-MWNT interact with the surfactant SDS.** It should be pointed out that the basic structure of the nanotubes is not affected (2<sup>nd</sup> peak), whereas their outer surface is affected (1<sup>st</sup> and 3<sup>rd</sup> peaks). This is the first report of this phenomenon.

## 5. EXPERIMENTAL

### 5.1. The Sensor

In order to measure the thermal conductivity of the nanofluid, a transient hot-wire instrument was assembled. According to the transient hot-wire technique, the temporal rise of a thin wire immersed in a test material, initially at thermal equilibrium, is observed following the application of a step voltage across the wire. The wire acts as a heat source and produces a time-dependent temperature field within the test material. When measurements are carried out in such a way as to minimize radiative effects and the material is isotropic with temperature-independent thermal conductivity, density, and heat capacity, the temperature gradient in the wire, subscript “w”, and the fluid, subscript “f”, are described by the equations

$$\text{Tantalum wire} \quad \rho_w C p_w \frac{\partial T_w}{\partial t} = \lambda_w \left[ \frac{\partial^2 T_w}{\partial x^2} + \frac{\partial^2 T_w}{\partial y^2} \right] + \frac{q}{a^2} \quad (1)$$

$$\text{Fluid} \quad \rho_f C p_f \frac{\partial T_f}{\partial t} = \lambda_f \left[ \frac{\partial^2 T_f}{\partial x^2} + \frac{\partial^2 T_f}{\partial y^2} \right] \quad (2)$$

where  $T$  is the absolute temperature [K],  $t$  is the time [s],  $\rho$  is the density [ $\text{kg}\cdot\text{m}^{-3}$ ],  $C_p$  is the heat capacity at constant pressure [ $\text{kJ}\cdot\text{kg}^{-1}\cdot\text{K}^{-1}$ ],  $q$  is the heat generated per unit length [ $\text{W}\cdot\text{m}^{-1}$ ] and  $a$  is the wire radius [m].

To perform measurements in nanofluids, it is essential that dimensions are kept as small as possible, owing to the high cost of the nanotubes. The geometry of the transient hot wire employed here for the measurement of the thermal conductivity of nanofluids is shown in Fig. 6. Two identical wires differing only in length are employed and the

temporal change of their resistance difference is recorded. This arrangement allows measurement of the resistance change of a finite segment of an infinite long wire [10]. The wires shown in Fig. 6, are made of tantalum, and have a diameter of  $25\ \mu\text{m}$ , and lengths of 3 and 7 cm respectively. They are spot-welded to 0.5-mm-diameter tantalum wires, which are held by small stainless-steel supports attached to a 2-mm-thick tantalum rod. This arrangement ensures that as the temperature changes, the wire remains always under tension as it has the same linear expansion coefficient as its support. The 0.5-mm-diameter tantalum wires are electrically insulated from the stainless-steel supports with the use of Teflon sleeves. The two wires are placed in a pressure vessel to perform measurements under pressure or in a glass cylinder for measurements in atmospheric pressure. In both cases, the internal diameter of the enclosure is 15 mm.

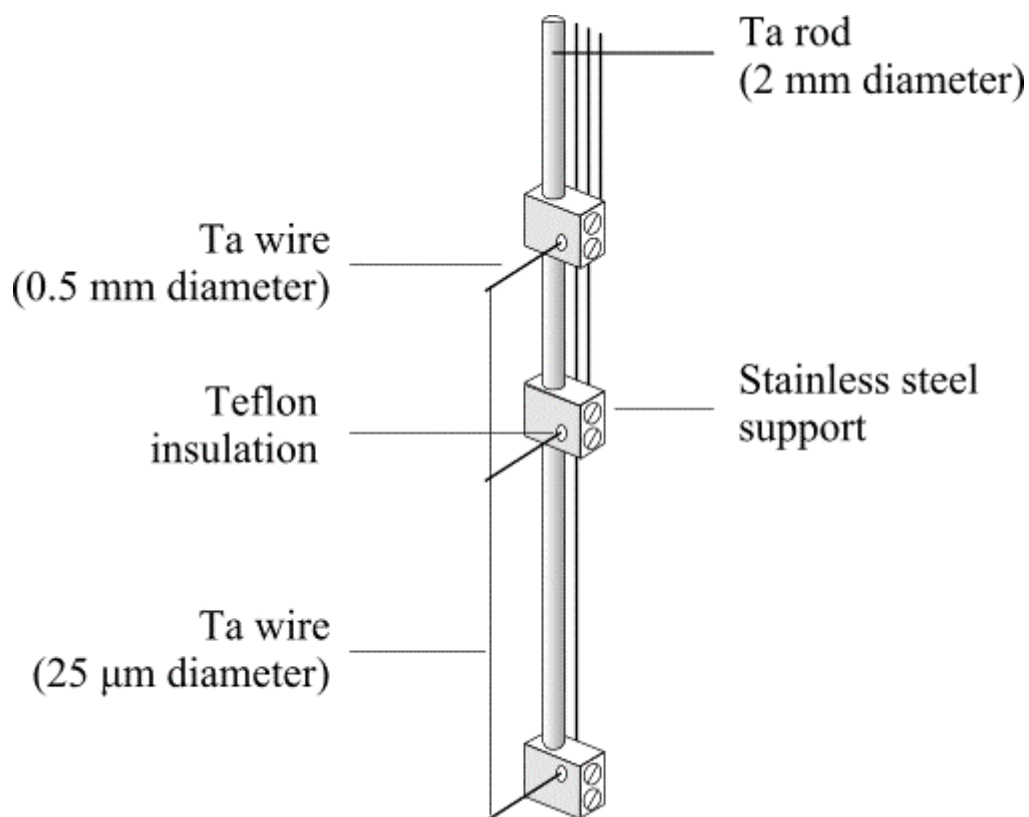


**Figure 6.** Wires Sensor

The wires were anodized in situ to form tantalum pentoxide, which is an electrical insulator. To ensure the stability of the oxide layer on both wires [11], a bias was applied to them by means of a DC supply so that the wires are positive with respect to the vessel, which is itself maintained at ground potential. This arrangement also provides the means of registering the leakage current from the wires to the vessel through the fluid at all times. This registered leakage current through the nanofluid was always less than  $1\ \mu\text{A}$ .

The wires are heated by an electrical current passing through them producing temperature rises between 3 and 4 K which are measured during the period 2ms to 1s. A computer-controlled Wheatstone bridge is employed, in order to heat the wires and measure their resistance at the same time, as described in detail elsewhere [12]. Employing a finite-element analysis to solve the aforementioned equations, the thermal conductivity,  $\lambda$ , and the product (density  $\times$  specific heat),  $(\rho C_p)$ , of the suspension are uniquely determined from the five hundred measurements of the temperature rise accumulated during one run.

The standard uncertainty of the thermal conductivity instrument employed is estimated to be about 0.5%, as confirmed also by measuring the thermal conductivity of pure water. However, due to the non-uniformity and complexity of the suspensions we prefer to quote a standard uncertainty of better than 2%.

## 5.2. Validation of Technique

In order to test the new sensor and the technique employed, the sensor was placed in water at 298.15 K and the thermal conductivity,  $\lambda$ , and the product  $(\rho C_p)$  measured directly on an absolute basis. The values are in excellent agreement with the literature values provided by the work of the Subcommittee on Transport Properties of the International Union of Pure and Applied Chemistry who have proposed a standard value for the viscosity of water having an uncertainty of 0.5% [13].

## 5.3. Thermal Conductivity Measurements

The results of the thermal conductivity measurements are shown in Fig. 7. The total homogenization time was employed as the abscissa. As already discussed, three groups of suspensions were prepared, resulting in the two curves in Fig. 7. **The maximum thermal conductivity enhancement measured was 38%.**

Group A suspensions showed the highest enhancement of the thermal conductivity. It is of interest to remind that Group A suspensions have nanotubes of length of more than 50  $\mu\text{m}$ , while Group B has nanotubes of length of less than 5  $\mu\text{m}$  and Group C of length less than 3  $\mu\text{m}$ . Furthermore, we also note:

a) Effect of SDS concentration.

It can be seen that the difference in SDS concentration has really no apparent significance for the thermal conductivity of the suspension.

b) Effect of homogenization time

As it is apparent in Fig. 7, increasing the homogenization time clearly reduced the enhancement of the thermal conductivity of the suspension. Examining SEM images showed that this fact is related to the breakage and thus the reduction in the length of the nanotubes. This remark is in agreement with Liu *et al.* [14].

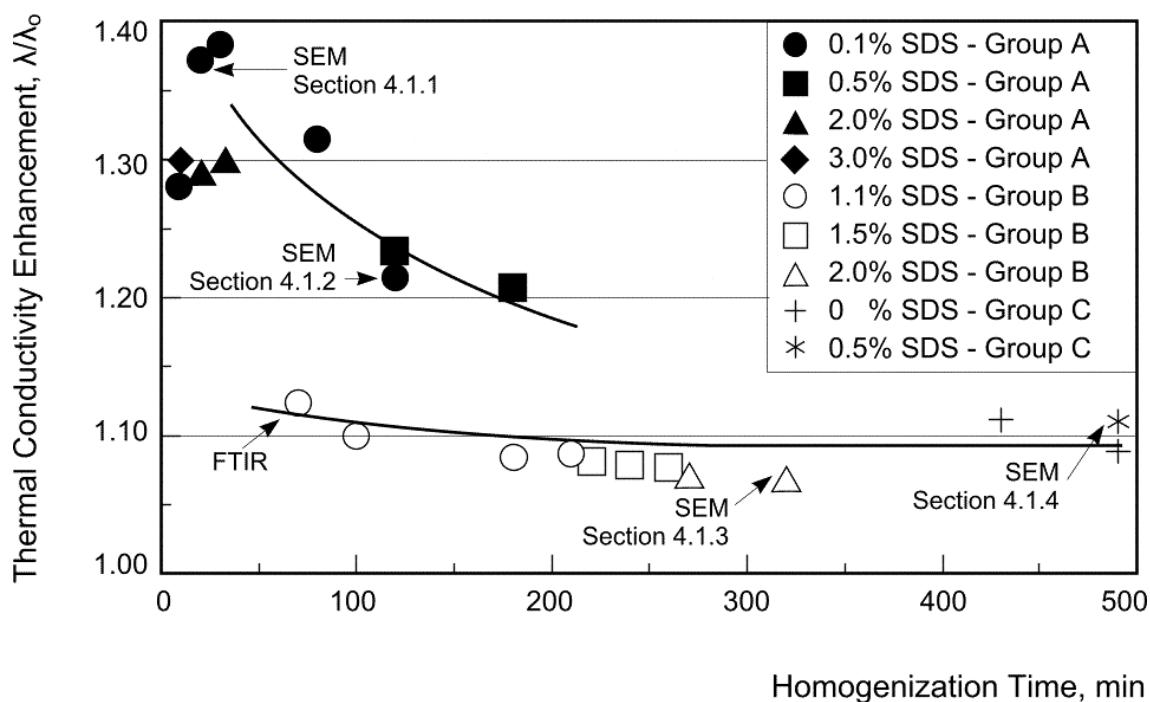


**Figure 7.** Effect of homogenization time and SDS content in a 0.6%vol suspension in water.

Hence, it seems that the length or perhaps the ratio of length to diameter of the C-MWNT is the dominant factor in the enhancement of the thermal conductivity of the suspensions. Computer simulations that will be reported elsewhere, also reinforce this observation.

Finally, it should be pointed out that, the nanotubes employed from MER-Corporation have a wide distribution of outer and core diameters, lengths and number of graphitic sheets. This fact may account for the different results in relation to Choi *et al* [6], who observed a much higher thermal conductivity enhancement.

## 6. CONCLUSIONS

The thermal-conductivity enhancement of 0.6% volume suspensions of C-MWNT in water with SDS as the dispersant, was investigated. Two main conclusions were drawn from the experiments and verified by the SEM analysis. These are:

- the enhancement of the thermal conductivity is increased, the longer the nanotubes are or the larger their ratio of length/diameter is.
- SDS is probably a suitable dispersant.

The highest thermal conductivity enhancement observed was 38%. A dispersant is certainly needed, and it seems that SDS is a good choice. It would be interesting to examine more substances as alternative dispersants, since they appear to be necessary.

## ACKNOWLEDGMENTS

The work could not be carried out without the help of MER-Corporation that provided the nanotubes. The authors are also indebted to E. Tsilika for carrying out the SEM analysis, Ch. Lioutas for the TEM analysis, O. Kamona for the FTIR analysis and S. Asimopoulos for carrying out the Raman analysis.

## REFERENCES

1. S. Iijima, *Nature* **354**:56 (1991).
2. H. Dai, N. Franklin, and J. Han, *Appl. Phys. Lett.* **73**:1508 (1998).
3. J. Cummings and A. Zettl, *Science* **289**:602 (2000).
4. P. Kim and C. M. Lieber, *Science* **286**:2148 (1999).
5. S. J. Tans, A. R. M. Verschueren, and C. Dekker, *Nature* **393**:49 (1998).
6. S. U. S. Choi, Z. G. Zhang, W. Yu, F. E. Lockwood, and E. A. Grulke, E. A., *Appl. Phys. Lett.* **79**:2252 (2001).
7. X. Zhao and Y. Ando, *Jpn. J. Appl. Phys.* **37**:4846 (1998).
8. H. Jantoljak, J.-P. Salvetat, L. Forro, C. Thomsen, *Appl. Phys. A* **67**:113 (1998).
9. C. Thomsen, S. Reich, H. Jantoljak, I. Loa, K. Syassen, M. Burghard, G. S. Duesberg, and S. Roth, *Appl. Phys. A* **69**:309 (1999).
10. J. Kestin and W. A. Wakeham, *Physica* **92A**:102 (1978).
11. M. J. Assael, E. Karagiannidis, and W. A. Wakeham, *Int. J. Thermophys.* **13**:735 (1992).
12. M. J. Assael, M. Dix, K. Gialou, L. Vozar, and W. A. Wakeham, *Int. J. Thermophys.* **23**:615 (2002).
13. M. L. V. Ramires, C. A. Nieto de Castro, R. A. Perkins, *Int. J. Thermophys.* **25**:269 (1993).
14. J. Liu, A. G. Rinzler, H. Dai, J. H. Hafner, R. K. Bradley, P. J. Boul, A. Lu, T. Iverson, K. Shelimov, C. B. Huffman, F. Rodriguez-Macias, Y-S. Shon, T. R. Lee, D. T. Colbert, and R. E. Smalley, R. E., *Science* **280**:1253 (1998).